ACS Catalysis

Letter

Cite This: ACS Catal. 2019, 9, 8867−8871

pubs.acs.org/acscatalysis

Switching on a Nontraditional Enzymatic Base—Deprotonation by Serine in the *ent*-Kaurene Synthase from *Bradyrhizobium japonicum*

Meirong Jia,[†,⊥] Yue Zhang,[‡,⊥] Justin B. Siegel,[*,‡,§,¶] Dean J. Tantillo,[*,‡] and Reuben J. Peters[*,†]

[†]Roy J. Carver Department of Biochemistry, Biophysics & Molecular Biology, Iowa State University, Ames, Iowa 50011, United States

[‡]Department of Chemistry, University of California-Davis, Davis, California 95616, United States

[§]Department of Biochemistry and Molecular Medicine, University of California-Davis, Davis, California 95616, United States

[¶]Genome Center, University of California-Davis, Davis, California 95616, United States

Supporting Information

ABSTRACT: Terpene synthases often catalyze complex carbocation cascade reactions. It has been previously shown that single-residue switches involving replacement of a key aliphatic residue with serine or threonine can "short-circuit" such reactions that are presumed to act indirectly via dipole stabilization of intermediate carbocations. Here a similar switch was found in the structurally characterized *ent*-kaurene synthase from *Bradyrhizobium japonicum*. Application of a recently developed computational approach to terpene synthases, *TerDockin*, surprisingly indicates direct action of the introduced serine hydroxyl as a catalytic base. Notably, this model suggests an alternative interpretation of previous results and potential routes toward reengineering terpene synthase activity more generally.

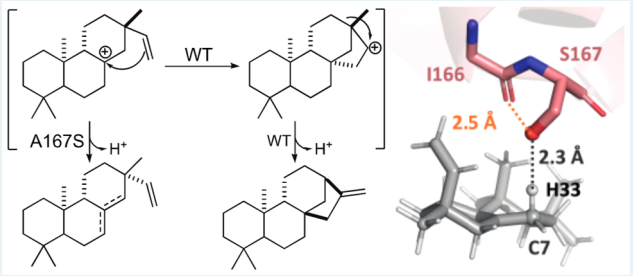

KEYWORDS: *biosynthesis, terpene synthases, enzymology, natural products, acid−base catalysis*

Terpene synthases produce intricate hydrocarbon backbones that underlie the structural diversity of the extensive family of terpenoid natural products.[1] This feat is accomplished by magnesium-assisted lysis of the allylic diphosphate ester in their isoprenyl substrates, which often triggers complex carbocation cascade reactions that are eventually terminated by deprotonation (or, occasionally, carbocation trapping by a nucleophile). To accommodate such reactive intermediates, the relevant portion of terpene synthase active sites have been observed to be largely nonpolar, composed of aliphatic and aromatic residues. Indeed, the perceived lack of side chains with suitable basicity has led to the hypothesis that the pyrophosphate anion coproduct ($^{-}$OPP) generally serves as the catalytic (general) base.[2]

Previous work has demonstrated that single residue changes can switch the product outcome in certain plant diterpene synthases.[3−11] Arguably the most interesting changes are those involving a key position that controls the complexity of the catalytic reaction. These enzymes are involved in labdane-related diterpenoid biosynthesis. Hence, they react with already bicyclic labdadienyl/copalyl diphosphate (CPP), carrying out initial cyclization to pimarenyl^{+} intermediates, which can be followed by further cyclization and/or rearrangement (e.g., Scheme 1). Strikingly, the presence of an aliphatic residue, typically alanine or isoleucine, leads to more complex reactions, while serine or threonine at the relevant key position

Scheme 1. Reactions Catalyzed by BjKS and A167S Mutant

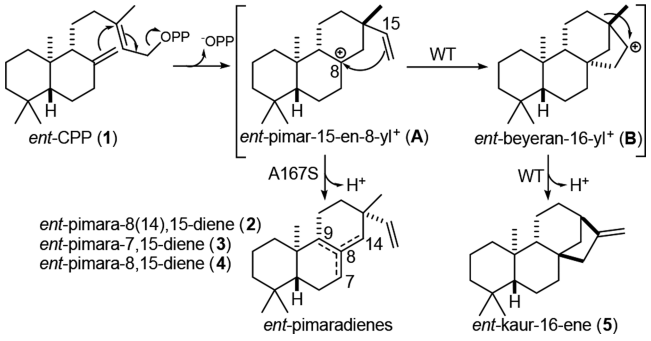

"short-circuits" the carbocation cascade, leading to production of pimaradienes. The key residue is hypothesized to be proximal to the carbocation in the pimarenyl^{+} intermediate, which continues to react in the presence of the aliphatic residue, but undergoes deprotonation when this is serine or threonine instead. However, based in large part on the perceived difficulty for such a nonactivated hydroxyl group to act as a catalytic base, these have been suggested to act via

Received: July 2, 2019
Revised: August 19, 2019
Published: August 27, 2019

DOI: 10.1021/acscatal.9b02783
ACS Catal. 2019, 9, 8867−8871

dipole stabilization of the initially formed pimarenyl$^+$ intermediate, enabling deprotonation (presumably by reorientation with respect to $^-$OPP).[12]

A number of labdane-related diterpene synthases also have been identified from bacteria. Of particular interest here is the *ent*-kaurene synthase from *Bradyrhizobium japonicum* (BjKS),[13] which has been shown to be involved in production of gibberellin phytohormones by this rhizobium.[14] Notably, high-resolution crystal structures have been determined for BjKS.[15] This revealed the expected nonpolar binding pocket for the hydrocarbon portion of its substrate, *ent*-CPP (**1**). While other residues were suggested to play particularly important roles in the catalyzed reaction, here alanine-167 was noted to exhibit intriguing parallels to a previously identified single-residue switch. In particular, A167 is located at a widely conserved helix-break (G1/2), just as observed for the critical alanine in the only plant diterpene synthase in which both a product switch (alanine to serine) has been identified[4] and that has a crystal structure currently available,[16] that is, the abietadiene synthase from *Abies grandis* (AgAS).

To investigate the hypothesis that A167 might be important in the (bi)cyclization and rearrangement reaction catalyzed by BjKS (Scheme 1), specifically continuation beyond initial cyclization of **1** to an *ent*-pimara-15-en-8-yl$^+$ intermediate (**A**) [e.g., to form the *ent*-beyeranyl$^+$ intermediate (**B**)], this residue was mutated to serine. The resulting BjKS:A167S mutant was observed to predominantly produce a roughly equal mixture of *ent*-pimara-8(14),15-diene (**2**) and *ent*-pimara-7,15-diene (**3**), resulting from immediate deprotonation of **A** (although no *ent*-pimara-8,15-diene, **4**, which also could be formed by deprotonation of **A**), along with small amounts of *ent*-kaurene (**5**), rather than the exclusive production of **5** exhibited by wild-type BjKS (Figure 1).

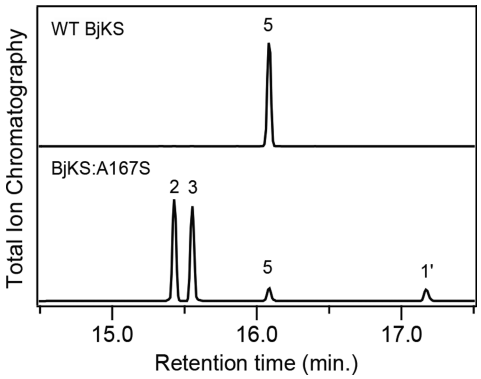

Figure 1. Chromatograms from GC-MS analysis of BjKS, either wild-type (WT) or A167S mutant, as indicated. Extracts from *E. coli* cultures engineered to produce **1** and coexpressing the indicated BjKS. Peaks are numbered as in the text, with **1′** indicating the dephosphorylated derivative of **1** produced by endogenous phosphatases (**1′**, *ent*-copalol; **2**, *ent*-pimara-8(14),15-diene; **3**, *ent*-pimara-7,15-diene; **5**, *ent*-kaur-16-ene), as identified by comparison to authentic standards.

Intriguingly, this single residue switch in BjKS differs from that found in plant *ent*-kaurene synthases (KSs), where the analogous residue is an isoleucine, with threonine substitution leading to predominant production of **2** and only small amounts of **3**.[3,6,8] Moreover, sequence alignment with AgAS suggests that this isoleucine does not fall into the G1/2 helix-break, but rather on the first turn of the G2 helix (i.e., four residues later).[4] This difference in location of the critical aliphatic residue between plant KSs and AgAS (which is representative of the family of diterpene synthases involved in conifer resin acid biosynthesis that are distinct from plant KSs[17]), has been attributed to their use of enantiomeric forms of CPP.[12] Regardless, it appears that **A** may be differentially oriented in BjKS than plant KSs, at least relative to the G1/2 helix, which is perhaps not surprising given that these share <15% sequence identity.[13]

To gain further insight into the role of the single-residue switch in BjKS, computational modeling was undertaken. First, density functional theory (DFT) calculations (PCM(water)-ωB97XD/6-311+G(d,p))[18] were carried out to compare the energies of the three possible deprotonation products of carbocation **A**. No significant difference in energy was found, however (relative energies in kcal/mol: **2**, +0.54; **3**, +0.73, **4**, 0.00), indicating that the observed product distribution is not the result of thermodynamic equilibration, nor its manifestation in transition state structures (TSSs) for deprotonation.

To gain further insight, the recently described *TerDockin* approach[19,20] was employed, using the Rosetta Molecular Modeling Suite.[21,22] To perform docking, all available X-ray crystal structures of BjKS were examined.[15] The structure with PDB code 4XLX was used because it had the most complete active site density (see Supporting Figure S1 for comparison). Hydrocarbon (carbocation) structures and the diphosphate-magnesium complex were docked into BjKS simultaneously. As no available BjKS structure contains a diphosphate-magnesium complex, the diphosphate conformation was extracted from the crystal structure 3P5R, the closest homologue of BjKS with such a complex present. Some conformations of carbocation structures were previously optimized using DFT calculations by Hong and Tantillo.[23] Carbocation conformers were identified using *Spartan 10* with the MMFF force field.[24] All conformers generated were then fully optimized using *Gaussian09*[25] with ωB97XD/6-31+g-(d,p). *TerDockin* was applied to both the wild-type BjKS and to the A167S mutant; results for the latter are discussed below, while results for the former can be found in the Supporting Information.

The conformer library of **A**, along with the diphosphate-magnesium complex, was docked into the BjKS:A167S structure to examine the relative positions of the carbocation center and S167. The first ionization step involves bond breaking between a diphosphate oxygen and the terminal carbon of **1**, leading to two possible carbocation-diphosphate ion pair orientations—the terminal carbon near to one or the other oxygen—since only two diphosphate oxygens protrude into the active site; these were examined separately during the docking simulation (Figure 2A; see the Supporting Information for details on the chemically meaningful constraints applied during docking).

As described above, simple alkene stability arguments do not rationalize the distribution of pimaradiene isomers observed. Moreover, the more selective production of **2** by the functionally analogous Ile → Thr mutation in the plant KSs argues against any significant effect from relative stability. Preliminary docking results suggested that *S167, rather than diphosphate, may act as the base for the deprotonation step to form the pimaradienes*. While an introduced histidine has been suggested to act as the catalytic base for production of cembrene A by the relevant mutant of taxadiene synthase,[26] it does not appear to have been previously suggested that a

DOI: 10.1021/acscatal.9b02783
ACS Catal. 2019, 9, 8867−8871

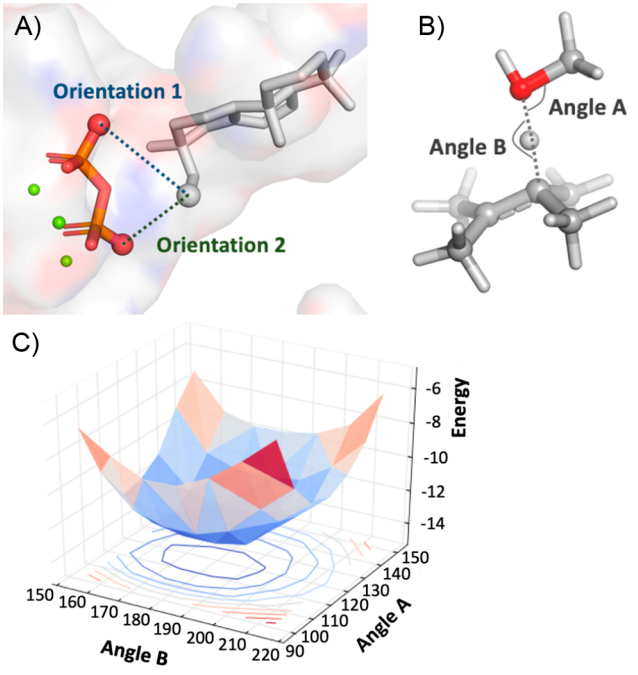

Figure 2. (A) Two diphosphate oxygen atoms to which the terminal carbon of the substrate may have been connected. (B) Model system to identify optimal angles of deprotonation by the S167 hydroxyl group: methanol and 2,3-dimethyl-2-butene. (C) 2D potential energy scan (vertical axis corresponds to relative electronic energies in kcal/mol; other axes correspond to angles from panel (B) in degrees) showing that the optimal angles are ∼120° for A and ∼180° for B.

hydroxyl containing residue can act as the catalytic base in terpene synthases. Nevertheless, the pK_a of a protonated alcohol is typically around −1 to −4,[27] while that of a typical carbocation lacking conjugation is less than −10,[28] suggesting that proton transfer from a carbocation to an alcohol is energetically reasonable. In addition, hydrogen atoms at C7, C9, and C14 all appeared to be reasonably close to the S167 oxygen. Consequently, we suspected that the hydroxyl group of S167 acts as a base and that certain $C_{carbocation}$−H−O and H−O−C_{Ser} angles in the deprotonation of TSS (Figure 2B) were preferred. Optimal angles for proton transfer during deprotonation were identified with DFT calculations on a model system (Figure 2B−C): ∼120° for H−O−C_{Ser} and ∼180° for $C_{carbocation}$−H−O. Constraints favoring these angles were then applied to the docking simulation (see Supporting Information for details and previous papers on terpene docking for the philosophy underpinning this approach and potential limitations[19,20]).

Docking simulations (25 000) for each of the two ion pair orientations and each of five possible deprotonation sites (C7 and C14 bear two hydrogen atoms, while C9 bears one) were then carried out (i.e., 250 000 total docking runs were performed). All docking results were combined and then filtered on the basis of satisfaction of constraints, total protein energy (the lowest 10% were kept), and interface energy (the lowest 5% were kept). Results are summarized in Figure 3 (see Supporting Information for details). In total, deprotonation at C7 (to form **2**) is predicted to be the most likely, with deprotonation at C14 (to form **3**) next most likely and deprotonation at C9 (to form **4**) unlikely (Figure 3A). The predicted 59:36:5 ratio for **2**:**3**:**4** is consistent with the experimental observation that **2** and **3** are formed in

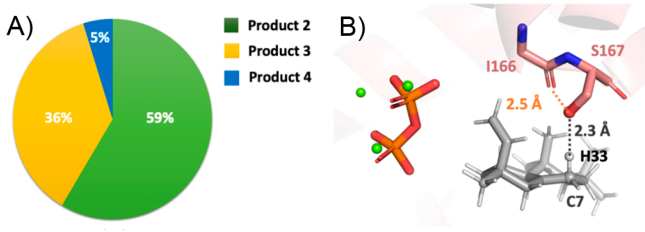

Figure 3. (A) Predicted relative amounts of pimaradiene products. All docking results are combined and filtered on the basis of satisfaction of constraints, total protein energy (the lowest 10% were kept), and interface energy (the lowest 5% were kept; see SI for additional details). (B) A representative pose predicted by docking (C7/Orientation 2/H33). The distance between the S167 oxygen and H33 is 2.3 Å. The distance between the I166 backbone carbonyl oxygen and the S167 oxygen is 2.5 Å.

comparable amounts, with slightly more **2** than **3**, while **4** is not observed, suggesting that the ability to approach the ideal TSS geometry during deprotonation plays a major role in product selectivity. Note also that the backbone carbonyl oxygen of I166 can hydrogen bond with the S167 hydroxyl group, further increasing the basicity of the Ser side chain (Figure 3B).

In summary, we suggest that the shortening of the BjKS carbocation cascade induced by the A167S substitution is due to direct action of the introduced alcohol as a catalytic base mediating premature deprotonation. Even beyond the implications for BjKS, our results further suggest that the previously identified analogous single residue product switches in plant diterpene synthases may operate in the same fashion; that is, the introduced serine or threonine may act as a catalytic base to terminate the carbocation cascade reaction. More importantly, appreciation of this ability to directly deprotonate carbocation intermediates immediately indicates that incorporation of hydroxyl containing side chains at appropriate locations provides a means to alter product outcome in enzymatic engineering of terpene synthases more generally, which will be explored in future work.

■ ASSOCIATED CONTENT

Supporting Information

The Supporting Information is available free of charge on the ACS Publications website at DOI: 10.1021/acscatal.9b02783.

Experimental details (PDF)
Intermediate **A** conformers (mol2 files) (ZIP)
Rosetta input files (PDB and text files) (ZIP)
Resulting poses (PDB files) (ZIP)

■ AUTHOR INFORMATION

Corresponding Authors

*E-mail for J.B.S.: jbsiegel@ucdavis.edu.
*E-mail for D.J.T.: djtantillo@ucdavis.edu.
*E-mail for R.J.P.: rjpeters@iastate.edu.

ORCID

Dean J. Tantillo: 0000-0002-2992-8844
Reuben J. Peters: 0000-0003-4691-8477

Author Contributions

⊥(M.J., Y.Z.) These authors contributed equally.

DOI: 10.1021/acscatal.9b02783
ACS Catal. 2019, 9, 8867−8871

Notes

The authors declare the following competing financial interest(s): R.J.P. is a member of the scientific advisory board for Manus Bio, Inc.

■ ACKNOWLEDGMENTS

The authors thank Terrance E. O'Brien for initial development of *TerDockin* and feedback on results obtained in this study. This work was supported by a grant (GM076324) from the National Institutes of Health (NIH).

■ REFERENCES

(1) Christianson, D. W. Structural and Chemical Biology of Terpenoid Cyclases. *Chem. Rev.* **2017**, *117*, 11570−11648.
(2) Pemberton, T. A.; Christianson, D. W. General Base-General Acid Catalysis by Terpenoid Cyclases. *J. Antibiot.* **2016**, *69*, 486−93.
(3) Xu, M.; Wilderman, P. R.; Peters, R. J. Following Evolution's Lead to a Single Residue Switch for Diterpene Synthase Product Outcome. *Proc. Natl. Acad. Sci. U. S. A.* **2007**, *104*, 7397−7401.
(4) Wilderman, P. R.; Peters, R. J. A Single Residue Switch Converts Abietadiene Synthase into a Pimaradiene Specific Cyclase. *J. Am. Chem. Soc.* **2007**, *129*, 15736−15737.
(5) Morrone, D.; Xu, M.; Fulton, D. B.; Determan, M. K.; Peters, R. J. Increasing Complexity of a Diterpene Synthase Reaction with a Single Residue Switch. *J. Am. Chem. Soc.* **2008**, *130*, 5400−5401.
(6) Jia, M.; Peters, R. J. Extending a Single Residue Swtich for Abbreviating Catalysis in Plant *ent*-Kaurene Synthases. *Front. Plant Sci.* **2016**, *7*, No. e1765.
(7) Keeling, C. I.; Weisshaar, S.; Lin, R. P. C.; Bohlmann, J. Functional Plasticity of Paralogous Diterpene Synthases Involved in Conifer Defense. *Proc. Natl. Acad. Sci. U. S. A.* **2008**, *105*, 1085−1090.
(8) Zerbe, P.; Chiang, A.; Bohlmann, J. Mutational Analysis of White Spruce (Picea glauca) *ent*-Kaurene Synthase (PgKS) Reveals Common and Distinct Mechanisms of Conifer Diterpene Synthases of General and Specialized Metabolism. *Phytochemistry* **2012**, *74*, 30−9.
(9) Kawaide, H.; Hayashi, K.; Kawanabe, R.; Sakigi, Y.; Matsuo, A.; Natsume, M.; Nozaki, H. Identification of the Single Amino Acid Involved in Quenching the *ent*-Kauranyl Cation by a Water Molecule in *ent*-Kaurene Synthase of *Physcomitrella patens*. *FEBS J.* **2011**, *278* (1), 123−33.
(10) Irmisch, S.; Muller, A. T.; Schmidt, L.; Gunther, J.; Gershenzon, J.; Kollner, T. G. One Amino Acid Makes the Difference: The Formation of *ent*-Kaurene and 16α-hydroxy-*ent*-Kaurane by Diterpene Synthases in Poplar. *BMC Plant Biol.* **2015**, *15*, 262.
(11) Jia, M.; O'Brien, T. E.; Zhang, Y.; Siegel, J. B.; Tantillo, D. J.; Peters, R. J. Changing Face: A Key Residue for the Addition of Water by Sclareol Synthase. *ACS Catal.* **2018**, *8*, 3133−3137.
(12) Zhou, K.; Peters, R. J. Electrostatic Effects on (Di)Terpene Synthase Product Outcome. *Chem. Commun.* **2011**, *47*, 4074−4080.
(13) Morrone, D.; Chambers, J.; Lowry, L.; Kim, G.; Anterola, A.; Bender, K.; Peters, R. J. Gibberellin Biosynthesis in Bacteria: Separate *ent*-Copalyl Diphosphate and *ent*-Kaurene Synthases in *Bradyrhizobium japonicum*. *FEBS Lett.* **2009**, *583*, 475−480.
(14) Nett, R. S.; Montanares, M.; Marcassa, A.; Lu, X.; Nagel, R.; Charles, T. C.; Hedden, P.; Rojas, M. C.; Peters, R. J. Elucidation of Gibberellin Biosynthesis in Bacteria Reveals Convergent Evolution. *Nat. Chem. Biol.* **2017**, *13*, 69−74.
(15) Liu, W.; Feng, X.; Zheng, Y.; Huang, C. H.; Nakano, C.; Hoshino, T.; Bogue, S.; Ko, T. P.; Chen, C. C.; Cui, Y.; Li, J.; Wang, I.; Hsu, S. T.; Oldfield, E.; Guo, R. T. Structure, Function and Inhibition of *ent*-Kaurene Synthase from Bradyrhizobium japonicum. *Sci. Rep* **2015**, *4*, 6214.
(16) Zhou, K.; Gao, Y.; Hoy, J. A.; Mann, F. M.; Honzatko, R. B.; Peters, R. J. Insights into Diterpene Cyclization from the Structure of the Bifunctional Abietadiene Synthase. *J. Biol. Chem.* **2012**, *287*, 6840−6850.
(17) Chen, F.; Tholl, D.; Bohlmann, J.; Pichersky, E. The Family of Terpene Synthases in Plants: A Mid-Size Family of Genes for Specialized Metabolism that is Highly Diversified Throughout the Kingdom. *Plant J.* **2011**, *66*, 212−29.
(18) Chai, J. D.; Head-Gordon, M. Long-Range Corrected Hybrid Density Functionals with Damped Atom-Atom Dispersion Corrections. *Phys. Chem. Chem. Phys.* **2008**, *10*, 6615−20.
(19) O'Brien, T. E.; Bertolani, S. J.; Tantillo, D. J.; Siegel, J. B. Mechanisticallly Informed Predictions of Binding Modes for Carbocation Intermediates of a Sesquiterpene Synthase Reaction. *Chem. Sci.* **2016**, *7*, 4009−4015.
(20) O'Brien, T. E.; Bertolani, S. J.; Zhang, Y.; Siegel, J. B.; Tantillo, D. J. Predicting Productive Binding Modes for Substrates and Carbocation Intermediates in Terpene Synthases-Bornyl Diphosphate Synthase as a Representative Case. *ACS Catal.* **2018**, *8*, 3322−3330.
(21) Alford, R. F.; Leaver-Fay, A.; Jeliazkov, J. R.; O'Meara, M. J.; DiMaio, F. P.; Park, H.; Shapovalov, M. V.; Renfrew, P. D.; Mulligan, V. K.; Kappel, K.; Labonte, J. W.; Pacella, M. S.; Bonneau, R.; Bradley, P.; Dunbrack, R. L., Jr.; Das, R.; Baker, D.; Kuhlman, B.; Kortemme, T.; Gray, J. J. The Rosetta All-Atom Energy Function for Macromolecular Modeling and Design. *J. Chem. Theory Comput.* **2017**, *13*, 3031−3048.
(22) Leaver-Fay, A.; Tyka, M.; Lewis, S. M.; Lange, O. F.; Thompson, J.; Jacak, R.; Kaufman, K.; Renfrew, P. D.; Smith, C. A.; Sheffler, W.; Davis, I. W.; Cooper, S.; Treuille, A.; Mandell, D. J.; Richter, F.; Ban, Y. E.; Fleishman, S. J.; Corn, J. E.; Kim, D. E.; Lyskov, S.; Berrondo, M.; Mentzer, S.; Popovic, Z.; Havranek, J. J.; Karanicolas, J.; Das, R.; Meiler, J.; Kortemme, T.; Gray, J. J.; Kuhlman, B.; Baker, D.; Bradley, P. ROSETTA3: An Object-Oriented Software Suite for the Simulation and Design of Macromolecules. *Methods Enzymol.* **2011**, *487*, 545−74.
(23) Hong, Y. J.; Tantillo, D. J. Formation of Beyerene, Kaurene, Trachylobane, and Atiserene Diterpenes by Rearrangements that Avoid Secondary Carbocations. *J. Am. Chem. Soc.* **2010**, *132*, 5375−86.
(24) Shao, Y.; Molnar, L. F.; Jung, Y.; Kussmann, J.; Ochsenfeld, C.; Brown, S. T.; Gilbert, A. T.; Slipchenko, L. V.; Levchenko, S. V.; O'Neill, D. P.; DiStasio, R. A., Jr.; Lochan, R. C.; Wang, T.; Beran, G. J.; Besley, N. A.; Herbert, J. M.; Lin, C. Y.; Van Voorhis, T.; Chien, S. H.; Sodt, A.; Steele, R. P.; Rassolov, V. A.; Maslen, P. E.; Korambath, P. P.; Adamson, R. D.; Austin, B.; Baker, J.; Byrd, E. F.; Dachsel, H.; Doerksen, R. J.; Dreuw, A.; Dunietz, B. D.; Dutoi, A. D.; Furlani, T. R.; Gwaltney, S. R.; Heyden, A.; Hirata, S.; Hsu, C. P.; Kedziora, G.; Khalliulin, R. Z.; Klunzinger, P.; Lee, A. M.; Lee, M. S.; Liang, W.; Lotan, I.; Nair, N.; Peters, B.; Proynov, E. I.; Pieniazek, P. A.; Rhee, Y. M.; Ritchie, J.; Rosta, E.; Sherrill, C. D.; Simmonett, A. C.; Subotnik, J. E.; Woodcock, H. L., III; Zhang, W.; Bell, A. T.; Chakraborty, A. K.; Chipman, D. M.; Keil, F. J.; Warshel, A.; Hehre, W. J.; Schaefer, H. F., III; Kong, J.; Krylov, A. I.; Gill, P. M.; Head-Gordon, M. Advances in Methods and Algorithms in a Modern Quantum Chemistry Program Package. *Phys. Chem. Chem. Phys.* **2006**, *8*, 3172−3191.
(25) Frisch, M. J.; Trucks, G. W.; Schlegel, H. B.; Scuseria, G. E.; Robb, M. A.; Cheeseman, J. R.; Scalmani, G.; Barone, V.; Petersson, G. A.; Nakatsuji, H.; Li, X.; Caricato, M.; Marenich, A.; Bloino, J.; Janesko, B. G.; Gomperts, R.; Mennucci, B.; Hratchian, H. P.; Ortiz, J. V.; Izmaylov, A. F.; Sonnenberg, J. L.; Williams-Young, D.; Ding, F.; Lipparini, F.; Egidi, F.; Goings, J.; Peng, B.; Petrone, A.; Henderson, T.; Ranasinghe, D.; Zakrzewski, V. G.; Gao, J.; Rega, N.; Zheng, G.; Liang, W.; Hada, M.; Ehara, M.; Toyota, K.; Fukuda, R.; Hasegawa, J.; Ishida, M.; Nakajima, T.; Honda, Y.; Kitao, O.; Nakai, H.; Vreven, T.; Throssell, K.; Montgomery, J. A., Jr.; Peralta, J. E.; Ogliaro, F.; Bearpark, M.; Heyd, J. J.; Brothers, E.; Kudin, K. N.; Staroverov, V. N.; Keith, T.; Kobayashi, R.; Normand, J.; Raghavachari, K.; Rendell, A.; Burant, J. C.; Iyengar, S. S.; Tomasi, J.; Cossi, M.; Millam, J. M.; Klene, M.; Adamo, C.; Cammi, R.; Ochterski, J. W.; Martin, R. L.; Morokuma, K.; Farkas, O.; Foresman, J. B.; Fox, D. J. *Gaussian 09*; Gaussian, Inc.: Wallingford, CT, 2016.
(26) Ansbacher, T.; Freud, Y.; Major, D. T. Slow-Starter Enzymes: Role of Active-Site Architecture in the Catalytic Control of the

DOI: 10.1021/acscatal.9b02783
ACS Catal. 2019, 9, 8867−8871

Biosynthesis of Taxadiene by Taxadiene Synthase. *Biochemistry* **2018**, *57*, 3773−3779.
(27) Deno, N. C.; Turner, J. O. The Basicity of Alcohols and Ethers. *J. Org. Chem.* **1966**, *31*, 1969−1970.
(28) McCormack, A. C.; More O'Ferrall, R. A.; O'Donoghue, A. C.; Rao, S. N. Protonated Benzofuran, Anthracene, Naphthalene, Benzene, Ethene, and Ethyne: Measurements and Estimates of pK(a) and pK(R). *J. Am. Chem. Soc.* **2002**, *124*, 8575−8583.

DOI: 10.1021/acscatal.9b02783
ACS Catal. 2019, 9, 8867−8871